Arabian Journal of Chemistry (2020) 13, 5966–5977

King Saud University

Arabian Journal of Chemistry

www.ksu.edu.sa
www.sciencedirect.com

ORIGINAL ARTICLE

Gold nanoparticles synthesized with *Poria cocos* modulates the anti-obesity parameters in high-fat diet and streptozotocin induced obese diabetes rat model

Wansen Li [a], Hong Wan [b], Shuxun Yan [b], Zhao Yan [b], Yalin Chen [b], Panpan Guo [b], Thiyagarajan Ramesh [c], Ying Cui [d,*], Lei Ning [d]

[a] *Department of General Medicine, Zhumadian Central Hospital, Zhumadian, Henan, 463000, China*
[b] *Department of Endocrinology, The First Affiliated Hospital of Henan University of CM, Zhengzhou City, Henkan Province 450000, China*
[c] *Department of Basic Medical Sciences, College of Medicine, Prince Sattam Bin Abdulaziz University, Al-Kharj 11942, Saudi Arabia*
[d] *Department of Endocrinology, Jinan Central Hospital Affiliated to Shandong University, No. 105, Jiefang Road, Lixia District, Jinan City, Shandong Province 250013, China*

Received 7 February 2020; accepted 25 April 2020
Available online 6 May 2020

KEYWORDS

Diabetes;
Obesity;
High fat diet;
Poria cocos;
Gold nanoparticles

Abstract Obesity is a foremost health issue that affects about 1.6 million people out of which 400 million worldwide. Epidemiological evidences prove obesity is the primary cause for various metabolic ailments e.g. diabetes. *Poria cocos* possess extensive biological actions, for instance, antioxidant, anti-inflammatory, antitumor, immunomodulatory actions. The primary limitation of all phytomedicine was their poor bioavailability hence in this investigation, we bio-fabricated the gold nanoparticles from *Poria cocos* aqueous extract and inspected their potency to treat obesity. Obese rat model were produced via fed the young female rats with high fat food for 8 weeks regimen. Further to confirm the potency of *Poria cocos* gold nanoparticles against obesity induced metabolic disorders we treated obese rats with low dose streptozotocin in the conclusion of the investigational time. The synthesis of *Poria cocos* gold-nanoparticles was evidenced via the UV-Spectroscopic study and characterized with SEM, TEM and EDAX studies. The anti-obesity actions of *Poria cocos* gold-nanoparticles were investigated by estimating the glucose profile, kidney markers, lipid profile, inflammatory cytokines, adipocyte markers, antioxidants in the *Poria cocos* gold nanoparticles trea-

* Corresponding author.
E-mail addresses: cuiyingxinxin896@sina.com (Y. Cui), ninglei197415@sina.com (L. Ning).
Peer review under responsibility of King Saud University.

Production and hosting by Elsevier

https://doi.org/10.1016/j.arabjc.2020.04.031

ted obese rats. To confirm the *Poria cocos* gold nanoparticles role on inhibiting the obesity induced metabolic disorders we analyzed the histopathological changes in cardiac tissues. Our physical characterization confirms the synthesized *Poria cocos* gold nanoparticles assure the distinctions of influential nanoparticles to be utilized for the treatment. The results from biochemical and histopathological analysis confirms *Poria cocos* gold nanoparticles is a persuasive antidiabetic, anti-inflammatory, antioxidant, anti-obesity drug. Overall our results authentically confirm *Poria cocos* gold nanoparticles is a potent anti-obesity drug and it also protects from obesity induced metabolic disorders.

1. Introduction

Obesity is a one among the foremost health concerns worldwide which don't limit itself to particular gender, age, ethnicity etc. (Wahl et al., 2017). All around the world about 1.6 million people were considered to be overweight out of which 400 million are adults and 40 million children were tend to be obese (Mutiso et al., 2014). The deregulated carbohydrate, fat metabolism in adipose tissue is primary causative agent of obesity (Travers and McCarthy, 2011). Epidemiological evidences prove obesity is the primary cause for various metabolic ailments, for example, diabetes, hypertension and cardiovascular complications (Lavie and Milani, 2003; Poirier et al., 2006). It also causes non alcoholic fatty liver, degenerative disease, asthma, arthritis, PCOD etc. (Tilg and Moschen, 2006). Obesity patients were currently treated with drugs that modulates fat and carbohydrate metabolism and they also targets the adipocytes to synthesis satiety hormones (Padwal and Majumdar, 2007). These drugs on long term medication leads to various side effects which are more worsen than the complication of obesity itself. Bariatric surgeries which once yielded a promising results in randomized trial also doesn't shown proven outcome in most of the obese patients. Hence it is essential to develop a potent therapeutic agent to overcome the obesity and its related metabolic disorders (Adams et al., 2007; Sjöström et al., 2007).

Phytomedicine which posses hypoglycemic, hypolipidemic, antioxidant properties are the potent alternative for current allopathic drugs (Marles and Farnsworth, 1995 Oct 1). Numerous researches were targeted on the pharmacological properties of plants but the research on phytochemicals obtained from mushrooms were limited. *Poria cocos* are one such saprophytic fungus which belongs to the family polyporaceae botanically named with different synonyms such as *Wolfiporia extensa*; *Wolfiporia cocos* (Lindner and Banik, 2008; Esteban, 2009). *Poria cocos* extracts possess various medicinal properties it is used to treat hyperglycemia. In vivo treatment with methanolic *Poria cocos* extract in streptozocin treated diabetes induced mice shown antihyperglycemic effect (Li et al., 2011). It also showed antihyperglycemic effect in obese mice with non insulin dependent diabetes model (Sato et al., 2002).

In vitro potency of phytomedicine is remarkable whereas in the case of *in vivo* treatment it is less efficient due to their lipophilic nature and poor bioavailability. Nanotechnology renders an effective remedy to overcome the hindrance in herbal medication. Nanoparticles synthesized with noble metals such as silver and gold have proven to be possess various applications in the fields of medical diagnosis, therapy (Llevot and Astruc, 2012; Zhou et al., 2015), targeted drug delivery (Wang et al., 2011; Tiwari et al., 2011), biosensors (Li et al., 2011). Nanoparticles (NPs) were synthesized using various techniques such as physical, chemical and biological (Gwynne, 2013; Zeng et al., 2018; Gan et al., 2020; Cai et al., 2018; Libutti et al., 2010). Biologically synthesized nanoparticles are ecofriendly, biocompatible and can be preferred to be prescribed for medications (Liu et al., 2016; Huang et al., 2018; Shi et al., 2017). NPs secured a unique place among the researchers, which owing to their distinctive physic-chemical properties (Liu et al., 2014; Huang et al., 2017; Huang et al., 2017). Gold nanoparticles were extensively utilized in traditional medicine against numerous chronic ailments due to its medicinal applications. Gold nanoparticles are more efficient than the other nanoparticles hence it is widely used in the field of cancer treatment since it possess high biocomptibility, drug efficacy and relatively low toxicity (Zhang et al., 2017). The green synthesis method was effective, inexpensive and reliable to develop nanomedicines (Iravani, 2011). In this current investigation, we fabricated the gold-nanoparticles by utilizing the aqueous extract of *Poria cocos* and inspected their antiobesity properties in high fat diet supplemented animal replica.

Diet play key role in induction of obesity in humans, high fat intake has proven to make both humans and animals obese (Jequier, 2002; Warwick and Schiffman, 1992). Rodents are the classical models of obesity which mimics the exactly like humans. High fat fed rats shown increased visceral adiposity, deregulated lipid and carbohydrate metabolism, increased inflammatory cytokines which closely resembles to the condition of obese patients (Sclafani and Springer, 1976). Obesity is a foremost influencing cause of insulin resistance type-II diabetes mellitus (Al-Goblan et al., 2014; Jung and Choi, 2014). Hence we assessed the efficacy of *Poria cocos* gold nanoparticles on high fat diet fed obese diabetes induced rats.

2. Materials & methods

2.1. Chemicals

2.1.1. ***Poria cocos*** *extract preparation*

Poria cocos were collected, rinsed with de-ionized water then dehydrated in air at shady place until got dehydrated completely. The shade dried Poria cocos were chopped and pulverized in a sterile condition using a mechanical blender. 100 g powdered *Poria cocos* were immersed in 1 l of sterile distilled water and boiled for three hours. The extract was filtered with 0.45 μm Whatman sift paper and then resulting filtrate was aliquoated, stored at −20 °C until used for additional analysis.

2.2. Synthesis of PC-AuNP

To the 95 ml of 1 mM Gold(III) chloride trihydrate solution, 5 ml of *Poria cocos* aqueous extract was mixed via drop by drop manner and stirred well and incubated at 37 °C for 15 min. The formation of *Poria cocos* Gold-nanoparticles (PC-AuNP) was observed by colour transform from gold to deep violet and finally red wine colour reveals the formation of PC-AuNP. The solution was then centrifuged at 16000 rpm for 25 min at 4 °C. The precipitated gold nanoparticles were separated and rinsed twice with distilled water. The synthesized PC-AuNP were then dried overnight at 37 °C and stored at −20 °C.

2.3. Characterization of PC-AuNP

2.3.1. Ultraviolet (UV)-Visible Spectroscopic study

The synthesis of PC-AuNP was evidenced by the UV–Visible spectroscopic study through spectrophotometer (Shimadzu UV-1650). The colour intensity of synthesized PC-AuNP was measured between the wavelengths 200 to 800 nm.

2.4. Surface morphology analysis

The surface morphology of bio-synthesized PC-AuNP was assessed through High-resolution Scanning Electron microscopy and High-resolution Transmission microscopy (TEM). The PC-AuNP sample were positioned on to the copper painted grid, permitted to dehydrate and then subjected to scanning electron microscope (SEM) analysis using FEI Quanta FEG 200 HRSEM equipped with energy dispersive X-ray (EDAX) analysis. TEM analysis was performed with JEO 2010 High resolution TEM instrument operated at an accelerating voltage f 200 keV. The image was assessed with ImageJ software to measure the particle size distribution, 200 particles from different TEM images were measured to detect the particle size.

2.5. Cell viability assay by MTT assay

The cytotoxity of PC-AuNP was investigated through the MTT assay. The normal cell line (Vero) was loaded in the 96-well plates at 5×10^4 cell/well and incubated for 24 h at 37 °C. Then the Vero cells were treated with the various dose of PC-AuNP (10–100 µg/ml). Then the MTT solution was added to the each wells and again incubated for 4 h at 37 °C. After that the medium was eliminated and the 100 µl of DMSO was added to liquefy the developed formazan crystals. Finally, the absorbance was measured at 570 nm by using microplate reader (Mosmann, 1983).

2.6. In vivo analysis

2.6.1. Animals

Healthy female Wistar rats 6–9 weeks aged, weighing 200–220 g was bought in the institutional animal house. The rats were acclimatized in the standard laboratory condition of 24 ± 3 °C, 50–60% humidity with 12 h light/dark cycle for a week. The bedding and cages of the rats were changed periodically. The rats were supplemented with standard pellet diet along with water ad libidum. Whole experimental treatments done in this experiment was permitted by institutional ethical committee. All rats were treated with highest care and concern every possible means were followed to minimize the discomfort to rats.

3. Experimental design

All the rats were alienated into five groups with six rats in each. Group-I rats were treated with standard pellet diet consisting of 11% fat, Group-II rats fed with high fat diet consisting of 42% of fat content (Lard, Coconut oil and Olive oil) for 8-weeks. Group-III rats induced with diabetes, and administered with high fat diet for 8-weeks and on the last day of treatment period, and the rats were injected intraperitoneally with streptozotocin (30 mg/kgbwt) dissolved on 0.01 M citrate-buffer (pH-4.5) (Holmes et al., 2015). Diabetes induction was studied via evaluating blood glucose through glucose oxidase reagent strip. Rats having blood glucose more than 250 mg/dl were considered to be diabetic. Group IV are low dose nanoparticles treated rats. The obese diabetes induced diabetes was treated with 25 mg/kg bwt of biosynthesised PC-AuNPs for 30 days. Group V are high dose nanoparticles treated rats. The obese diabetes induced diabetes was treated with 50 mg/kg bwt of biosynthesised PC-AuNPs for 30-days. After that the rats were fasted for overnight and euthanized on the next day morning. Blood was collected by heart puncture for biochemical analysis and the heart was dissected for further histological analysis.

3.1. Anthropometrical analysis

The induction of obesity was assessed by determining the anthropometrical parameters in rats. The bodyweight of the control and experimental rats were assessed daily and the average gain of bodyweight was calculated at the end of the investigational schedule. The body mass index was calculated via measuring the weight and length of the rats.

$$Body\ mass\ index\ (BMI) = Body\ Weight(g)/Length^2(cm^2)$$

3.2. Determination of blood glucose and insulin levels

The blood glucose and glycosylated hemoglobin (HbA1C) levels of the control and investigational rats were assessed using the colorimetric assay kits (CATALOG# 81693, CATALOG# 80300 respectively) procured from Crystal Chem, USA. Plasma insulin levels and serum advanced glycation end products were measured using ELISA kits procured from ThermoFisher Scientific, USA (Catalog # ERINS), and MyBioSource, USA (AGE, MBS700464) respectively.

3.3. Determination of urea and creatinine levels

The blood urea (Catalog #: K375) and creatinine (Catalog #: K625) statuses were examined with the aid of commercial colorimetric assay kits bought from BioVision, USA. The protocols were followed in accordance to the manufacturer guidelines and the end product absorbance ranges were inspected at 570 nm using microplate reader. The levels of urea

and creatinine were calculated using standard reference curve values.

3.4. Lipid profile estimation

The total lipid profile, total cholesterol, triglycerides, HDL cholesterol, LDL cholesterol, VLDL cholesterol and free fatty acids of control and investigational rats were examined via assay kits (ab65390) procured form Abcam, USA. Total cholesterol was estimated using the whole serum whereas for HDL cholesterol estimation the sample was precipitated as per the manufacturer's protocol using the precipitation buffer. LDL and VLDL cholesterol levels were measured using the below mentioned formula

$$\text{LDL(mg/dl)} = \text{TC} - \text{HDL} - \text{TG}/5$$

$$\text{VLDL(mg/dl)} = \text{TG}/5$$

The triglyceride (TG) statuses were investigated through the commercial colorimetric Triglyceride Quantification Assay Kit (ab65336), Abcam, USA. The end point reaction was measured at OD 570 nm using microplate reader.

3.5. Atherogenic and coronary risk index measurement

The atherongenic index of plasma was investigated in accordance to the procedure of Onat et al. (2010)

$$\text{Atherogenic index of plasma} = \text{Triglycerides/HDL cholesterol}$$

Coronary risk index was calculated using the formula (Abbott et al., 1988)

$$\text{Cornary risk index} = \text{Total cholesterol/HDL cholesterol}$$

3.6. Estimation of liver marker enzymes

Liver functioning emzymes alanine transaminase (ALT), aspartate transaminase (AST) and alkaline phosphatase (ALP) were estimated via colorimetric procedure using commercial assay kits.

3.7. Estimation of inflammatory markers

Inflammatory markers Tumor necrosis factor-α (TNF-α), Interleukins-1β (IL-1β) and Interleukin-6 (IL-6) were examined through the commercial ELISA kits bought from MyBiosource, USA. Serum samples were mixed to the TNF-α (MBS355371), IL-1 β (MBS774854), IL-6 (MBS495037) antibody precoated ELISA plates accordingly followed by the adding of biotin conjugated antibodies. The colour change of end product produced via the TMB substrates was investigated at the absorbance of 450 nm and the statuses of inflammatory cytokines were calculated using the standard curve reference values.

3.8. Estimation of adipocyte cell markers

Adipocytes cells synthesized markers leptin, adiponectin and resistin were examined in the control and investigational rats via the commercial ELISA test kits leptin (MBS774908), Adiponectin (MBS774139) and resistin (MBS013451) procured from MyBioSource, USA. The end product absorbance was inspected at 450 nm and the levels were determined using the standard curve reference values.

3.9. Estimation of oxidative stress markers

Thiobarbituric acid reactive substances (TBARS), byproduct of lipid peroxidation were measured using the protocol of Yagi (1978). TBARS are measured as MDA equivalent, the sample was heated along with TBA solution which forms a pink chormogen. The absorbance was measured at 532 nm and the statuses of TBARS were determined. Values are expressed nmole/mg protein. Reduced glutathione levels were examined via the Ellman (Yagi, 1978) technique (Ellman, 1959), the sulfhydryl groups exist in the reduced glutathione unites with the 5,5′dithio2-nitro benzoic acid to produce colour strength which was determined at 415 nm. Values are illustrated μg of reduced glutathione formed /min.

3.10. Histopathological analysis

The control and experimental rats heart tissue was fixed in 4% formaldehyde for 48 h and processed with different concentration of ethanol and xylene. The processed was then embedded in paraffin wax and then manually sectioned into 4 μm sections using microtome. The sections were dewaxed and then stained with hematoxylin and eosin. Then the slides were inspected beneath the light microscope and imaged to study the histopathological alterations.

3.11. Statistical analysis

The results were assessed using one-way ANOVA afterwards the post-hoc test Bonferroni tests via the GraphPad Prism Tool. The results were expressed as mean ± SEM, $p < 0.05$ was regarded as statistically significant.

4. Results

4.1. Characterization of PC-AuNPs

4.1.1. UV–Visible Spectroscopic study of PC-AuNPs

The synthesis of PC-AuNPs were observed by the colour change from golden yellow colour to red wine colour within 15 min after addition Gold(III) chloride trihydrate to the aqueous extract of *Poria cocos*. Further the synthesis was evidenced with UV–Vis Spectrosopic study were the maximum absorption peak of *Poria cocos* extract was observed at 238–240 nm, whereas the surface Plasmon resonance band of PC-AuNPs was observed at 540 nm (Fig. 1).

4.1.2. Surface morphology analysis of PC-AuNP

The size and morphology of the biosynthesized PC-AuNP were assessed using SEM (Fig. 2A) and TEM (Fig. 2B) analysis. The HR-TEM images shows spherical form and they are poly-dispersed; the nanoparticles were typical size of 20 nm. EDAX study confirms the occurrence of gold nanoparticles via demonstrating distinctive peak and it also displayed weak

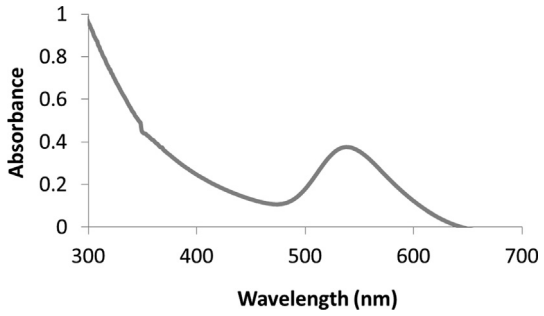

Fig. 1 Physical characterization of biosynthesized nanoparticles PC-AuNPs. UV-Spectroscopic surface Plasmon resonance peak of Poria cocos aqueous extract and biosynthesized PC-AuNPs.

carbon and oxygen peak that may because of the occurrence of other molecules bound to the surface of AuNP (Fig. 2C).

4.1.3. Cytotoxic effect of synthesized PC-AuNPs

The level of cytotoxicity of PC-AuNPs against the normal (Vero) cell lines were examined by using MTT assay and the result was illustrated in the Fig. 3. As mentioned in the Fig. 3, the PC-AuNPs were revealed no substantial toxicity to the normal (Vero) cell line. The PC-AuNPs were administered in different doses (10–100 µg/ml) and the 90 µg of PC-AuNPs were inhibited 50% of cell growth. Thus, the 90 µg of PC-AuNP was considered as IC_{50} dose.

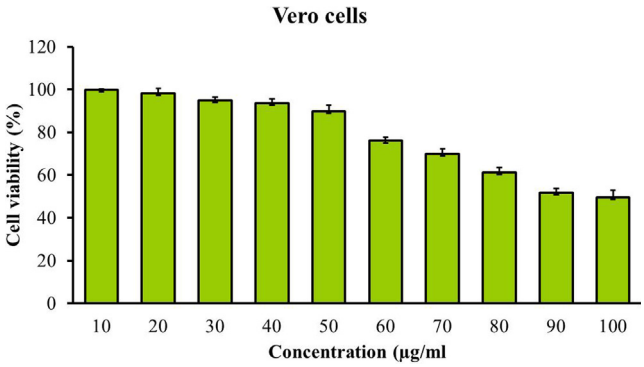

Fig. 3 Effect of PC-AuNP on the viability of normal cell (Vero) line. Values are expressed as means ± SEM for six independent observation of each group. $p \leq 0.05$ considered to be statistically significant.

4.1.4. Effect of PC-AuNP on weight gain and body mass index (BMI)

Fig. 4 A depicts the average weight gained by the control and experimental rats. Group II high fat diet rats (390 ± 7 g) shown significantly increased weight gain compared to the diabetes (290 ± 4 g) induced and gold nanoparticles treated rats (260 ± 2 g, 250 ± 5 g respectively). Body mass index was also considerably increased in high fat diet rats (1.7 ± 0.02) compared to the diabetic induced rats (1.39 ± 0.03). Compared to high fat diet and diabetes induced rats both the high and

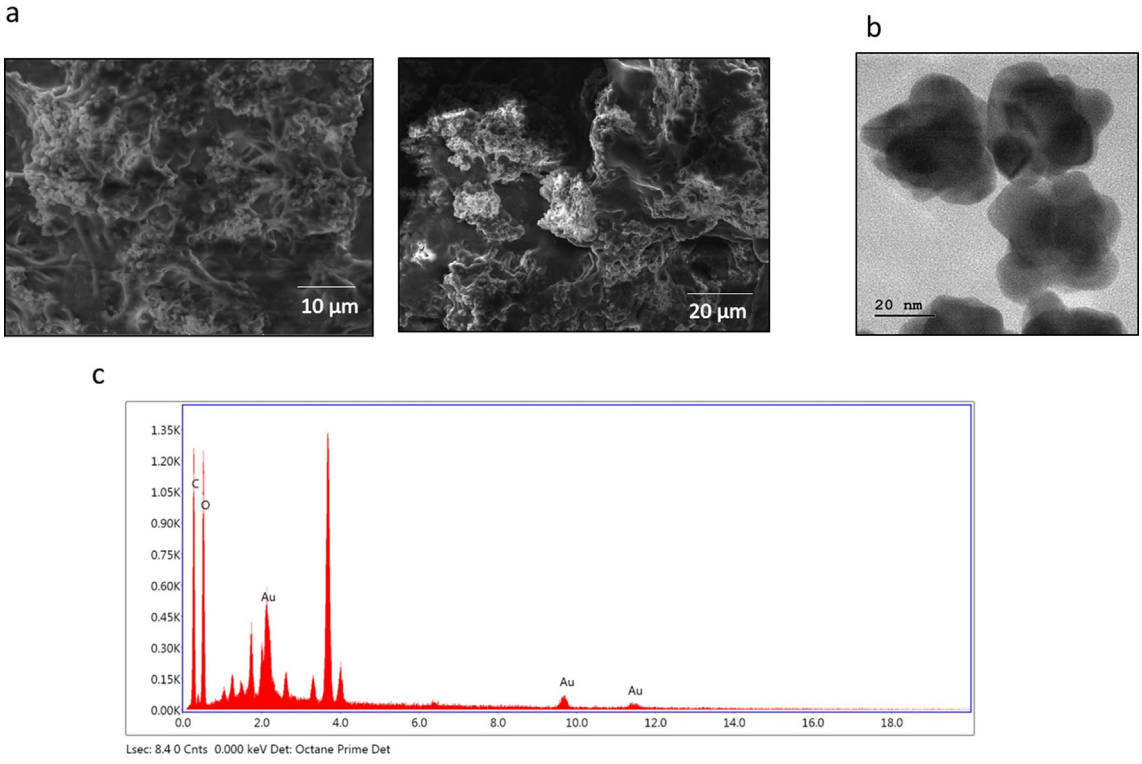

Fig. 2 Surface Morphology analysis of PC-AuNP. Scanning electron microscope photograph of biosynthesized PC-AuNPs (Fig. 2A), High resolution transmission electron microscope photograph of biosynthesized PC-AuNPs (Fig. 2B) and Energy dispersive X-ray analysis of biosynthesized PC-AuNPs (Fig. 2C).

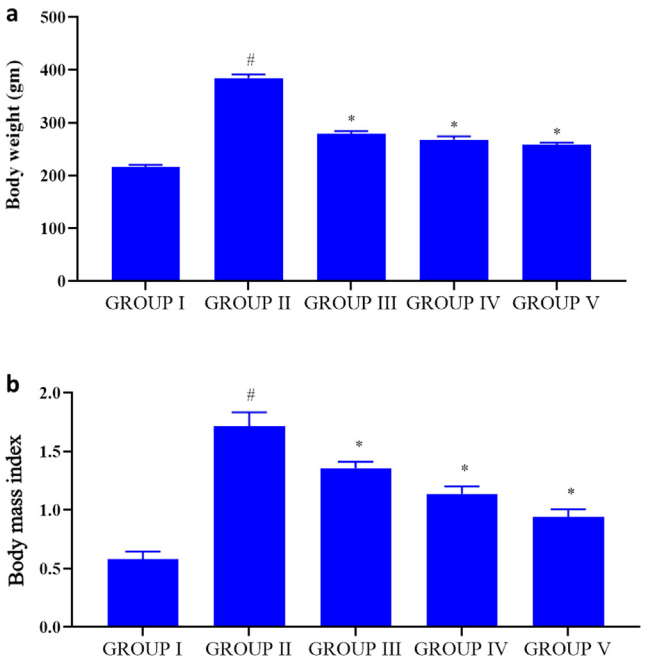

Fig. 4 Effect of PC-AuNP on weight gain & body mass index (BMI) on high fat diet fed diabetes induced. Values are expressed as means ± SEM for six independent observation of each group. $p \leq 0.05$ considered to be statistically significant.

low dose PC-AuNPs treated rats shown significantly decreased BMI (0.91 ± 0.04, 1.18 ± 0.02) (Fig. 4B).

4.2. Antidiabetic property of PC-AuNP

To assess the antidiabetic property of PC-AuNPs the blood glucose, insulin, glycosylated hemoglobin (HbA1C) and serum advanced glycation end products were measured. Compared to the diabetes induced rats (320 ± 8 mg/dl) the levels of blood glucose were drastically increased in high-fat diet stimulated rats (170 ± 10 mg/dl). High dose PC-AuNPs treated rats shown noticeably reduced blood glucose status (125 ± 5 mg/dl) while comparing it to the high-fat diet and diabetes induced rats (Fig. 5). Plasma insulin ranges were appreciably increased in control and high dose PC-AuNP treated rats compared to the high-fat diet and diabetes induced rats while the glycosylated hemoglobin and serum advanced glycation end products notably elevated in high-fat diet and diabetes stimulated rats.

4.3. Effect of PC-AuNPs on kidney markers

Fig. 6 illustrates the kidney markers like urea and creatinine statuses in control and investigational rats. Compared to control the urea level (85 ± 1.2 mmol/L) was reduced in high fat diet rats (52 ± 2.8 mmol/L) and diabetes induced rats (67 ± 2.5 mmol/L) whereas the creatinine (30 ± 2.4 g/L) statuses were elevated in high-fat diet rats (40 ± 1.8 g/L) and diabetes induced rats (38 ± 3.1 g/L). High dose PC-AuNPs treated rats shown comparatively equal levels of urea and creatinine as that of control rats.

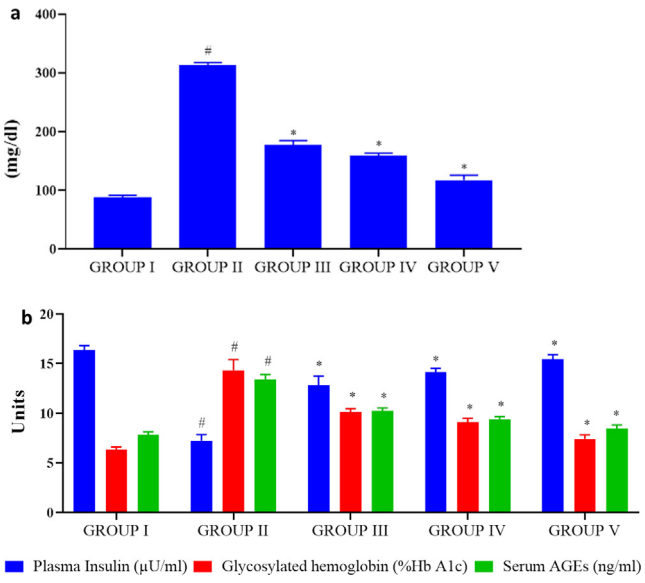

Fig. 5 Antidiabetic property of biosynthesized PC-AuNP on high fat diet fed diabetes induced rats. Blood glucose level in control and high fat diet fed diabetes induced rats treated with biosynthesized PC-AuNPs (Fig. 5A). Plasma insulin, glycosylated hemoglobin (HbA1C) and serum advanced glycation end products (AGE) were measured using commercially available ELISA kits (Fig. 5B). Values are expressed as means ± SEM for six independent observation of each group. $p \leq 0.05$ considered to be statistically significant.

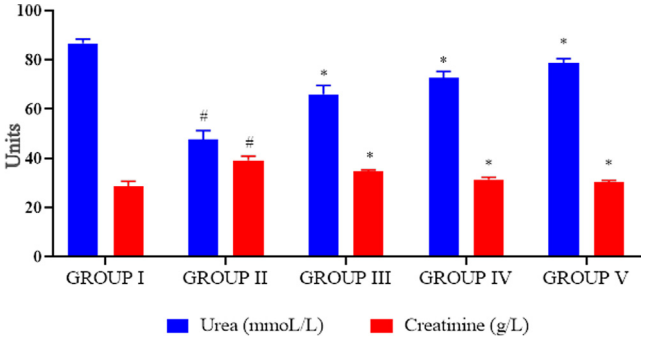

Fig. 6 Effect of biosynthesized PC-AuNPs on kidney markers of high fat diet fed diabetes induced rats. The kidney markers urea and creatinine levels in control and high fat diet fed diabetes induced rats treated with biosynthesized PC-AuNPs were measured using commercially available colorimetric assay kits. Values are expressed as means ± SEM for six independent observation of each group. $p \leq 0.05$ considered to be statistically significant.

4.4. Antilipidemic effect of PC-AuNPs

Total lipid profile consisting of total cholesterol, triglycerides, high density lipoprotein (HDL) cholesterol, low density lipoprotein (LDL) cholesterol, very low density lipoprotein (VLDL) cholesterol and free fatty acids of control and investigational rats were examined and depicted in Fig. 7A. The statuses of cholesterol, triglycerides, LDL cholesterol, VLDL cholesterol and free fatty acids were drastically elevated in

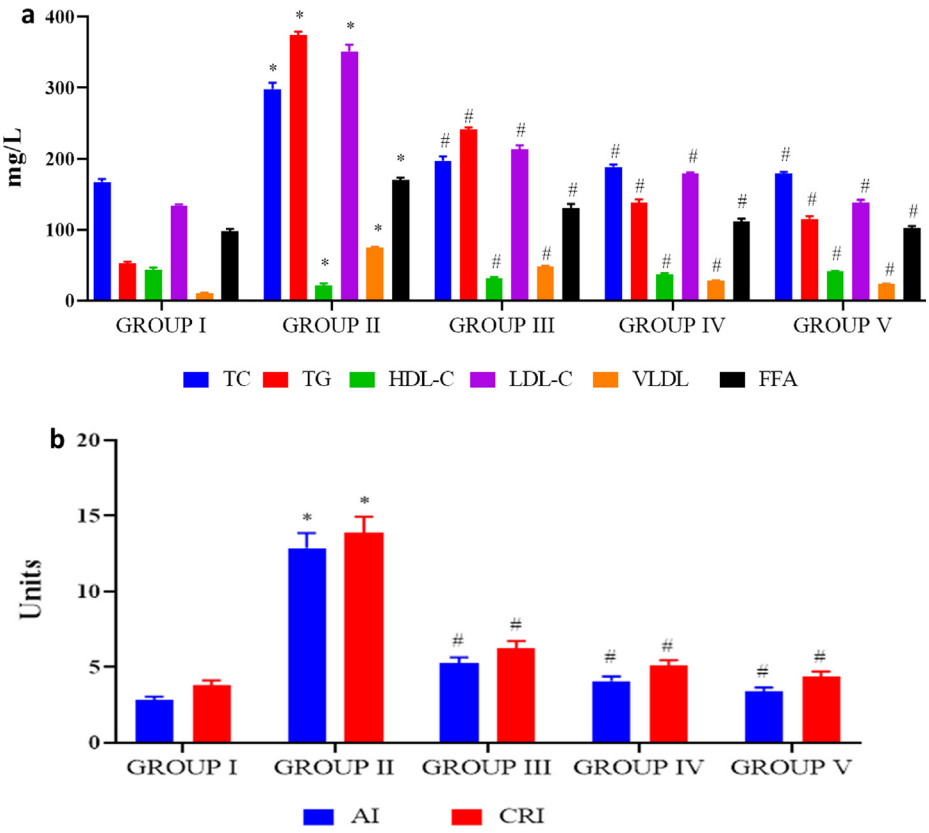

Fig. 7 Antilipidemic effect of biosynthesized PC-AuNPs on high fat diet fed diabetes induced rats. The total lipid profile total cholesterol, triglycerides, HDL cholesterol, LDL cholesterol, VLDL cholesterol and free fatty acids were measured in control and high fat diet fed diabetes induced rats treated with biosynthesized PC-AuNPs (Fig. 7A). Atherogenic index and coronary risk index were calculated using the levels of triglycerides, total cholesterol and HDL cholesterol estimated in control and high fat diet fed diabetes induced rats treated with biosynthesized PC-AuNPs (Fig. 7B). Values are expressed as means ± SEM for six independent observation of each group. $p \leq 0.05$ considered to be statistically significant.

high-fat diet treated group while comparing it to the PC-AuNPs and diabetes induced rats. Whereas the HDL-cholestrol levels notably reduced in high-fat diet treated group than the PC-AuNPs and diabetes induced rats. No significant variation was noted among the total lipid profile statuses between the control and high dose PC-AuNPs treated rats.

The atherogenic index and coronary risk index were drastically elevated in high-fat diet group rats than the other group rats. Both high and low dose PC-AuNP treatment in obese induced diabetic rats significantly decreased the atherogenic and coronary risk index (Fig. 7B).

4.5. Anti-inflammatory effect of PC-AuNPs

Fig. 8A represents the statuses of liver enzyme markers ALT, AST and ALP in control and experimental rats. The PC-AuNPs treated rats showed significantly decreased ranges of liver marker enzymes ALT, AST and ALP than the high-fat diet fed rats. No considerable variation was noted among the control and PC-AuNPs treated rat's liver enzyme levels. High fat diet induced inflammation were assessed by estimating the inflammatory cytokines TNF-α, IL-1 β, IL-6 levels in high fat diet and PC-AuNPs treated rats (Fig. 8B). IL-6 status was drastically elevated in high-fat diet rats than the diabetes induced rats treated with both low and high dose of PC-AuNPs. TNF-α, IL-1 β were also notably elevated in the high-fat diet rats whereas the PC-AuNPs treatment decreased the levels of inflammatory cytokines.

4.6. Anti-obesity effect of PC-AuNPs

Adipocytes plays a key role in promoting obesity related disorders, therefore we estimated the adipocyte markers leptin, resistin and adiponectin in control and investigational rats (Fig. 9). Leptin and resistin statuses were radically elevated in the high-fat diet fed rats whereas the adiponectin significantly decreased. Both the high and low dosage PC-AuNPs treatment significantly reduced the statuses of leptin, resistin and elevated the levels of adiponectin in high-fat diet fed diabetes induced rats.

4.7. Antioxidant effect of PC-AuNPs

Obesity increases the oxidative stress thereby leads to inflammation in high-fat diet fed rats. Hence we measured the statuses of TBARS and antioxidant reduced glutathione in control and investigational rats (Fig. 10A&B). TBARS levels were drastically elevated and reduced gluthathione status in

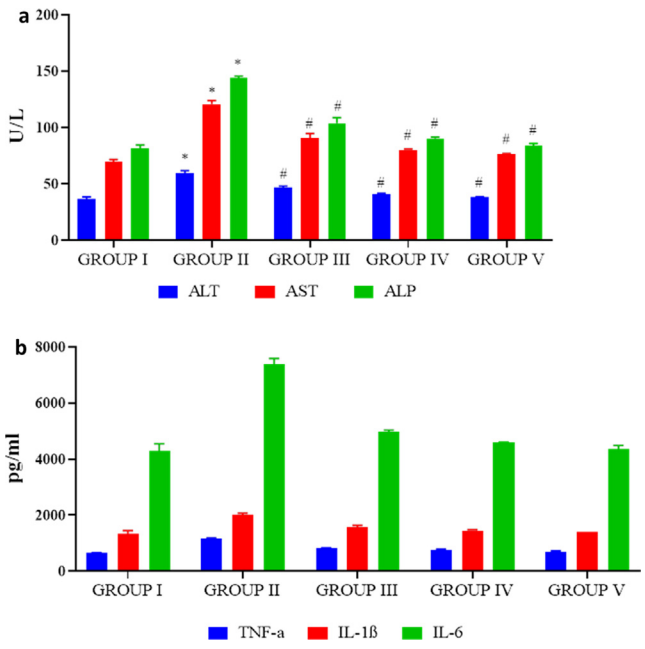

Fig. 8 Antiinflammatory effect of biosynthesized PC-AuNPs on high fat diet fed diabetes induced rats. The liver marker enzymes alanine aminotransferase (ALT), aspartate aminotransferase (AST) and alkaline phosphatase of control and high fat diet fed diabetes induced rats treated with biosynthesized PC-AuNPs were measured using commercially available colorimetric assay kits (Fig. 8A). Inflammatory cytokines TNF-α, IL-1β and IL-6 levels in control and high fat diet fed diabetes induced rats treated with biosynthesized PC-AuNPs were measured using commercially available ELISA kits. Values are expressed as means ± SEM for six independent observation of each group. $p \leq 0.05$ considered to be statistically significant.

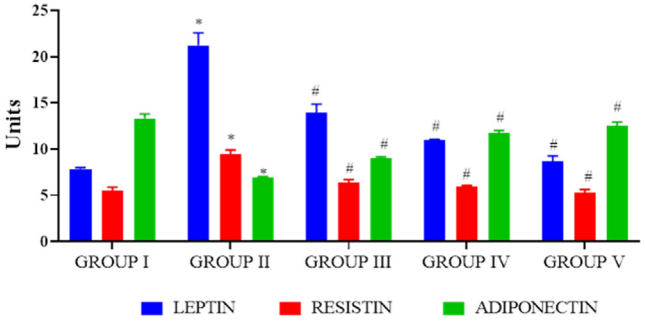

Fig. 9 Antiobesity effect of biosynthesized PC-AuNPs on high fat diet fed diabetes induced rats. The levels of adipocyte cell markers leptin, resistin and adiponectin were estimated in control and high fat diet fed diabetes induced rats treated with biosynthesized PC-AuNPs were estimated using commercially available ELISA kits. Values are expressed as means ± SEM for six independent observation of each group. $p \leq 0.05$ considered to be statistically significant.

high-fat diet fed rats whereas PC-AuNPs supplementation noticeably reduced the TBARS level and increased the reduced glutathione level in high-fat diet fed diabetes stimulated rats.

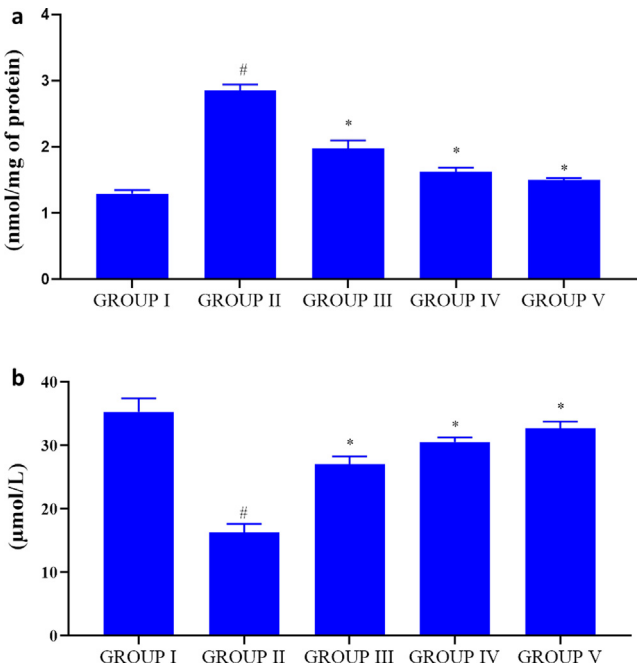

Fig. 10 Antioxidant effect of biosynthesized PC-AuNPs on high fat diet fed diabetes induced rats. The levels of oxidative stress marker TBARS (Fig. 10A) and antioxidant reduced glutathione (Fig. 10B) were measured in control and high fat diet fed diabetes induced rats treated with biosynthesized PC-AuNPs. Values are expressed as means ± SEM for six independent observation of each group. $p \leq 0.05$ considered to be statistically significant.

4.8. Effect of PC-AuNPs on cardiac muscles

Fig. 11 depicts the representative photomicrographs of control and PC-AuNPs treated high fat diet fed diabetes induced rats haematoxylin and eosin stained cardiac muscle tissue. Control (Fig. 11A) and low, high dose PC-AuNPs (Fig. 11D, Fig. 11E respectively) treated rats cardiac muscle tissue shown regular pattern of cardiac myofibres with oval shaped nuclei located centrally on the cardiomyocytes. Whereas irregular pattern of cardiac myofibres were observed in high-fat diet fed rats (Fig. 11B) and high-fat diet fed diabetes induced rats (Fig. 11C).

5. Discussion

Unhealthy life style practice was drastically increased in both developed and developing countries population. Malnourished or unhealthy diet intake, lack of physical exercise, addiction to alcohols, drugs were observed in most of the younger population (Farhud, 2015). Unhealthy life style leads to various health concerns one among them is obesity which ubiquitously affects global population without any discrimination of age, gender and ethnicity. High fat diet intake is the primary cause of visceral obesity which caused deregulated carbohydrate and lipid metabolism leading to infiltration of cytokines causing adipocytes inflammation, insulin resistance (Meneses and Flores, 2019). High fat diet fed obese rat models are the ideal obese models to study pathological changes which exactly mimic the condition of humans (Aguila and Mandarim-

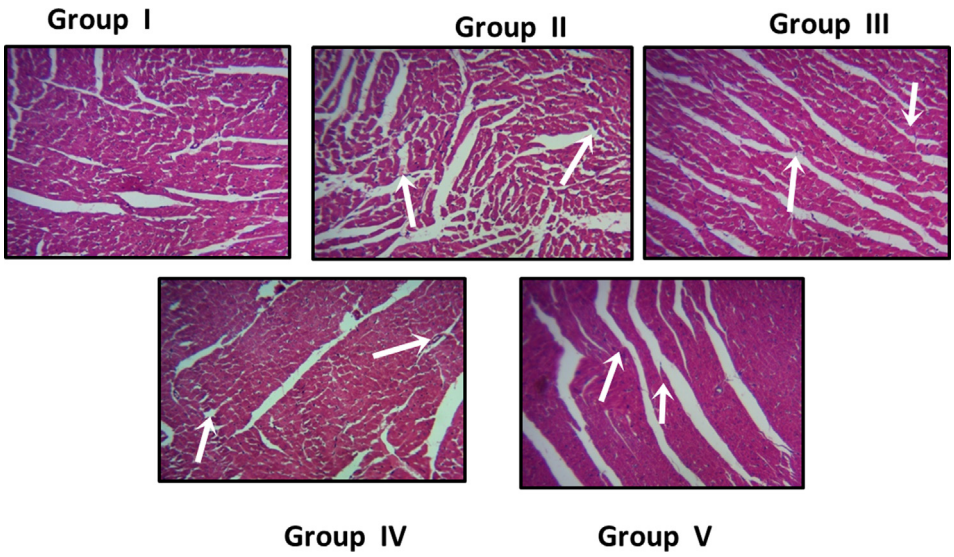

Fig. 11 Effect of biosynthesised on PC-AuNPs cardiac tissue histomorphometry on high fat diet fed diabetes induced rats. The cardiac tissues of control (Group I), low dose (Group IV), and high dose (Group V) of PC-AuNPs treated animal shows a regular pattern of cardiac myofibres with oval shaped nuclei located centrally on the cardiomyocytes. Whereas irregular pattern of cardiac myofibres were observed in high-fat diet fed rats (Group II) and high-fat diet fed diabetes induced rats (Group III).

de-Lacerda, 2003; Woods et al., 2003). The metallic nanoparticles were received a greater attention among the biomedical researchers duo to its exclusive properties (Liu et al., 2015; Shi et al., 2017). Therefore in this research investigation, we stimulated the obesity in rats with high-fat diet and also administered with low-dose of streptozotocin to also the potency of PC-AuNPs against the obesity induced to metabolic disorders. PC-AuNPs. PC-AuNPs effectively reduced average body weight gain and it also decreased the body mass index high fat diet fed rats (Fig. 4). Our results correlate with the previous epidemiological research where six weeks of Poria cocos treatment effectively reduced weight gain and body mass index in Portuguese population (Mendes, 2018).

Type2 diabetes is one of the most devastating complication of obesity which was observed in more than 171 million population and estimated to be increased to 360 million by the year 2030 (McKeigue et al., 1991; Tsai et al., 2011). Deposition of lipids in white adipocytes which prevents the lipids from peripheral tissue which are prone to insulin induced lipotoxicity and it also increases the hepatic gluconeogenesis via acetyl-CoA allosteric activity (Czech et al., 2013; Perry et al., 2015; Titchenell et al., 2016; Clerk et al., 2002). It also decreased the utilization of glucose by skeletal muscles via inhibiting the glucose transportation and metabolism (Karpe et al., 2011). Increased body mass index was reported to have positive correlation with insulin resistance; peripheral fat disruption increases the insulin sensitivity whereas it is decreased in visceral fat (Samane et al., 2006). In this current investigation, the high-fat diet fed rat shown increased level of plasma glucose, glycosylated heamoglobin and decreased levels of insulin which confirms the induction of diabetes whereas PC-AuNPs showed appreciably reduced of blood glucose levels. The anti-hyperglycemic activity of PC-AuNPs may be due to the phytochemicals dehydrotumulosic acid, dehydrotrametenolic acid and pachymic acid which enhanced insulin sensitivity in high-fat diet fed rats (Park et al., 2009).

Dyslipidemia is other pathologic condition observed in high-fat diet stimulated obesity were the adipocytes fails to oxidize the excessive fat leading to increased triglycerides and free fatty acids (Malloy and Kane, 2001). Triglycerides accumulates lipids in hepatic tissue thereby increases the insulin resistance whereas the HDL-cholestrol assists the excretion of lipids in bile from the hepatic tissue. The increased levels of triglycerides, LDL-cholestrol, free fatty acid and decreased levels of HDL-cholestrol is a positive indicator of atherosclerosis (Hertog et al., 1993). In the present study dyslipidemia condition was confirmed in high fat diet fed rats whereas the PC-AuNPs treatment significantly increased the HDL-cholestrol levels and decreased the levels of total cholesterol, triglycerides and free fatty-acids. The antihyperlipidemic and cardioprotective property of PC-AuNPs was confirmed with the atherogenic index and coronary risk index which are indicators of deregulated cholesterol metabolism (Chait et al., 1996; Ahima, 2006).

Adipocytes secretes adipokines like leptin, adiponectin, resistin and cytokines, i.e. interleukin 4, interleukin 6, tumour necrosis factor α which regulates the immunity in normal individual (Gannagé-Yared et al., 2006). Deregulated adipocytes secretion was reported in obese individuals cause's chronic inflammation leading to various metabolic syndromes (Considine et al., 1996). Hyperleptinemia (Maffei et al., 1995; Galler et al., 2007) and hypoadipnectinemia (Silha et al., 2003) were reported in the obese, type diabetes mellitus patients with increased body mass index. Leptin, hormone which regulates the apetite, glucose and lipid metabolism was drastically reduced in high-fat diet fed rats whereas the adiponectin hormone which increases the insulin sensitivity and posess anti-inflammatory property (Warne, 2003) was drastically reduced in high-fat diet fed rats. PC-AuNPs efficiently reduced the statuses of satiety hormones leptin and resistnin and elevated the levels of adiponectin this may be due to the anti-inflammatory property of PC-AuNPs.

Chronic inflammation was linked with obesity induction and other metabolic disease in obese individuals. Increased TNF- α cytokines levels were reported in both obesity induced type II diabetes mellitus as well as type I diabetes (Mandrup-Poulsen, 1996). Proinflammatory cytokine interleukin1 which is the early mediator of inflammation (Horn et al., 2000) and the interleukin6 that regulates energy homeostasis (Surmi and Hasty, 2008) was significantly increased in high-fat diet fed rats. The elevation in the inflammatory cytokines may be because of the increased adipocytes which activate the macrophage infiltration leading to subsequent activation of cytotoxic T cells and causing inflammation (Ríos, 2011). The decreased levels inflammatory cytokines in PC-AuNPs treated high-fat diet fed diabetes induced rats may be as a result of the anti-inflammatory property exhibited by the phytochemical triterpenes present in *Poria cocos* extract (Fonseca-Alaniz et al., 2007).

The increased levels of proinflammatory cytokines support the macrophages to generate free radicals causing oxidative stress in adipose tissue (Fantuzzi and Faggioni, 2000). In the present study high-fat diet elevated the TBARS level and reduced the antioxidant glutathione level which may be due to the hyperleptinemia and hypoadiponectinemia which increased the macrophage infiltration and secretion of proinflammatory cytokines (Pi-Sunyer, 2002). PC-AuNPs potent antioxidant effectively scavenged the free radicals and increased the antioxidant reduced glutathione thereby prevented the adipocytes from inflammation.

Obesity impairs functioning of major organs such as heart, kidney and liver. Nephropathy and non alcholic fatty liver are the frequent impediment caused by the obesity. Therefore in this investigation, we assessed the potency of bio-formulated PC-AuNP to protect liver and kidney from high fat diet induced complications. PC-AuNPs effectively increased the urea and creatinine status and decreased the levels of ALT, AST and ALP levels which prove PC-AuNPs has a potent antiobesity drug with nil side effects. Further to confirm the role of PC-AuNPs on atherosclerosis inhibition a major complication observed in most of the obese patients, histopathological analysis of cardia tissue of PC-AuNPs treated high diet fed diabetes induced rats was performed. Our results confirm that PC-AuNPs protects cardiac tissue from the complications induced by the high fat diet.

6. Conclusion

To conclude, we biosynthesized gold nanoparticle with saprophytic fungi Poria cocos used in traditional Chinese and Japanese medicine. Physical characterization with UV–Vis Spectroscopic anaylsis, SEM, HR-TEM and EDAX analysis confirms the PC-AuNPs is an ideal nanoparticle can be used for medication. *Invivo* analysis with high fat diet fed diabetes induced rats proves PC-AuNPs efficiently reduces the weight gain and body mass index. Biochemical analysis confirms PC-AuNPs potentially regulates glucose, lipid metabolism and it also inhibits the adipose tissue inflammation. PC-AuNPs scavenges oxidative stress and normalizes the satiety hormones thereby protected the high fat diet fed rats from hepatotoxicity, nephrotoxicity and atherosclerosis induction by the excessive fat intake. Overall, the outcomes of our study accurately proved that the PC-AuNPs is a promising anti obesity agent that not only prevents obesity but also obesity linked metabolic disorders.

Declaration of Competing Interest

The authors declare no conflict of interest.

References

Abbott, R.D., Wilson, P.W., Kannel, W.B., Castelli, W.P., 1988. High density lipoprotein cholesterol, total cholesterol screening, and myocardial infarction, The Framingham Study. Arteriosclerosis. 8 (3), 207–211.

Adams, T.D., Gress, R.E., Smith, S.C., Halverson, R.C., Simper, S.C., Rosamond, W.D., Lamonte, M.J., Stroup, A.M., Hunt, S.C., 2007. Longterm mortality after gastric bypass surgery. N. Engl. J. Med. 357, 753–761.

Aguila, M.B., Mandarim-de-Lacerda, C.A., 2003. Heart and blood pressure adaptations in Wistar rats fed with different high-fat diets for 18 months. Nutrition., 19347–19352

Ahima, R.S., 2006. Metabolic actions of adipocyte hormones: focus on adiponectin. Obesity (Silver Spring). 14 (1), 9–15.

Al-Goblan, A.S., Al-Alfi, M.A., Khan, M.Z., 2014. Mechanism linking diabetes mellitus and obesity. Diabetes Metab Syndr Obes. 7, 587–591.

Cai, G., Yu, Z., Ren, R., Tang, D., 2018. Exciton-plasmon interaction between AuNPs/Graphene nanohybrids and CdS quantum dots/TiO_2 for photoelectrochemical aptasensing of prostate-specific antigen. ACS Sens. 3, 632–639.

Chait, A., Brunzell, J.D., 1996. Diabetes, lipids, and atherosclerosis. In: LeRoith, D., Taylor, S.I., Olefsky, J.M. (Eds.), Diabetes Mellitus. Lippincott-Raven Publishers, Philadelphia, pp. 467–469.

Clerk, L.H., Rattigan, S., Clark, M.G., 2002. Lipid infusion impairs physiologic insulin-mediated capillary recruitment and muscle glucose uptake in vivo. Diabetes 51 (4), 1138–1145.

Considine, R.V., Sinha, M.K., Heiman, M.L., Kriauciunas, A., Stephens, T.W., Nyce, M.R., Ohannesian, J.P., Marco, C.C., McKee, L.J., Bauer, T.L., 1996. Serum immunoreactive-leptin concentrations in normal-weight and obese humans. N. Engl. J. Med. 334 (5), 292–295.

Czech, M.P., Tencerova, M., Pedersen, D.J., Aouadi, M., 2013. Insulin signalling mechanisms for triacylglycerol storage. Diabetologia 56 (5), 949–964.

Ellman, G.L., 1959. Tissue sulfhydryl groups. Arch. Biochem. Biophys. 82, 70–77.

Esteban, C.I., 2009. Interés medicinal de Poria cocos (= Wolfiporia extensa). Revista iberoamericana de micologia. 26 (2), 103–107.

Fantuzzi, G., Faggioni, R., 2000. Leptin in the regulation of immunity, inflammation, and hematopoiesis. J. Leukoc. Biol. 68 (4), 437–446.

Farhud, D.D., 2015. Impact of lifestyle on health. Iranian J. Public Health. 44 (11), 1442.

Fonseca-Alaniz, M.H., Takada, J., Alonso-Vale, M.I., Lima, F.B., 2007. Adipose tissue as an endocrine organ: from theory to practice. J. Pediatr. (Rio J). 83 (5), 192–203.

Galler, A., Gelbrich, G., Kratzsch, J., Noack, N., Kapellen, T., Kiess, W., 2007. Elevated serum levels of adiponectin in children, adolescents and young adults with type 1 diabetes and the impact of age, gender, body mass index and metabolic control: a longitudinal study. Eur. J. Endocrinol. 157 (4), 481–489.

Gan, D., Huang, Q., Dou, J., Huang, H., Chen, J., Liu, M., Wen, Y., Yang, Z., Zhang, X., Wei, Y., 2020. Bioinspired functionalization of MXenes ($Ti_3C_2T_X$) with amino acids for efficient removal of heavy metal ions. App. Surface Sci. 504, 144603.

Gannagé-Yared, M.H., Khalife, S., Semaan, M., Fares, F., Jambart, S., Halaby, G., 2006. Serum adiponectin and leptin levels in relation to the metabolic syndrome, androgenic profile and

somatotropic axis in healthy non-diabetic elderly men. Eur. J. Endocrinol. 155 (1), 167–176.
Gwynne, P., 2013. There's gold in them their bugs. Nature 495 (7440), S12–S13.
Hertog, M.G., Feskens, E.J., Hollman, P.C., Katan, M.B., Kromhout, D., 1993. Dietary antioxidant flavonoids and risk of coronary heart disease: the Zutphen Elderly Study. Lancet 342 (8878), 1007–1011.
Holmes, A., Coppey, L.J., Davidson, E.P., Yorek, M.A., 2015. Rat models of diet-induced obesity and high fat/low dose streptozotocin type 2 diabetes: effect of reversal of high fat diet compared to treatment with Enalapril or menhaden oil on glucose utilization and neuropathic endpoints. J. Diabetes Res. 2015, 307285.
Horn, F., Henze, C., Heidrich, K., 2000. Interleukin-6 signal transduction and lymphocyte function. Immunobiology 202 (2), 151–167.
Huang, Q., Liu, M., Mao, L., Xu, D., Zeng, G., Huang, H., Jiang, R., Deng, F., Zhang, X., Wei, Z., 2017. Surface functionalized SiO_2 nanoparticles with cationic polymers via the combination of mussel inspired chemistry and surface initiated atom transfer radical polymerization: Characterization and enhanced removal of organic dye. J. Colloid Interface Sci. 499 (1), 170–179.
Huang, Q., Liu, M., Chen, J., Wan, Q., Tian, J., Huang, L., Jiang, R., Wen, Y., Zhang, X., Wei, Y., 2017. Facile preparation of MoS_2 based polymer composites via mussel inspired chemistry and their high efficiency for removal of organic dyes. App. Sur. Sci. 419, 35–44.
Huang, L., Liu, M., Huang, H., Wen, Y., Zhang, X., Wei, Y., 2018. Recent advances and progress on melanin-like materials and their biomedical applications. Biomacromolecules 19 (6), 1858–1868.
Iravani, S., 2011. Green synthesis of metal nanoparticles using plants. Green Chem. 13 (10), 2638–2650.
Jequier, E., 2002. Pathways to obesity. Int. J. Obes. 26, S12–S17.
Jung, U.J., Choi, M.S., 2014. Obesity and its metabolic complications: the role of adipokines and the relationship between obesity, inflammation, insulin resistance, dyslipidemia and nonalcoholic fatty liver disease. Int. J. Mol. Sci. 15 (4), 6184–6223.
Karpe, F., Dickmann, J.R., Frayn, K.N., 2011. Fatty acids, obesity, and insulin resistance: time for a reevaluation. Diabetes 60 (10), 2441–2449.
Lavie, C.J., Milani, R.V., 2003. Obesity and cardiovascular disease: the Hippocrates paradox?. J. Am. Coll. Cardiol. 42 (4), 677–679.
Li, T.H., Hou, C.C., Chang, C.L., Yang, W.C., 2011. Anti-Hyperglycemic Properties of Crude Extract and Triterpenes from Poria cocos. Evid Based Complement Alternat Med. 2011, 128402.
Libutti, S.K., Paciotti, G.F., Byrnes, A.A., Alexander Jr., H.R., Gannon, W.E., Walker, M., Seidel, G.D., Yuldasheva, N., Tamarkin, L., 2010. Phase I and pharmacokinetic studies of CYT-6091, a novel PEGylated colloidal gold-rhTNF nanomedicine. Clin. Cancer Res. 16 (24), 6139–6149.
Lindner, D.L., Banik, M.T., 2008. Molecular phylogeny of Laetiporus and other brown rot polypore genera in North America. Mycologia 100 (3), 417–430.
Liu, Y., Ai, K., Lu, L., 2014. Polydopamine and its derivative materials: synthesis and promising applications in energy, environmental, and biomedical fields. Chem. Rev. 114 (9), 5057–5115.
Liu, M., Ji, J., Zhang, X., Zhang, X., Yang, B., Deng, F., Li, Z., Wang, K., Yang, Y., Wei, Y., 2015. Self-polymerization of dopamine and polyethyleneimine: novel fluorescent organic nanoprobes for biological imaging applications. J. Mater. Chem. B 3, 3476–3482.
Liu, M., Zang, G., Wang, K., Wan, Q., Tao, L., Zhang, X., Wei, Y., 2016. Recent developments in polydopamine: an emerging soft matter for surface modification and biomedical applications. Nanoscale. 8 (38), 16819–16840.
Llevot, A., Astruc, D., 2012. Applications of vectorized gold nanoparticles to the diagnosis and therapy of cancer. Chem. Soc. Rev. 41 (1), 242–257.
Maffei, M., Halaas, J., Ravussin, E., Pratley, R.E., Lee, G.H., Zhang, Y., Fei, H., Kim, S., Lallone, R., Ranganathan, S., 1995. Leptin levels in human and rodent: measurement of plasma leptin and ob RNA in obese and weight-reduced subjects. Nat. Med. 1 (11), 1155–1161.
Malloy, M.J., Kane, J.P., 2001. A risk factor for atherosclerosis: triglyceride-rich lipoproteins. Adv. Intern. Med. 47, 111–136.
Mandrup-Poulsen, T., 1996. The role of interleukin-1 in the pathogenesis of IDDM. Diabetologia 39 (9), 1005–1029.
Marles, R.J., Farnsworth, N.R., 1995. Antidiabetic plants and their active constituents. Phytomedicine 2 (2), 137–189.
McKeigue, P.M., Shah, B., Marmot, M.G., 1991. Relation of central obesity and insulin resistance with high diabetes prevalence and cardiovascular risk in South Asians. Lancet 337 (8738), 382–386.
Mendes, L.C., 2018. Effective fuling (Poria Cocos) for the treatment of obesityInt. J. Complement Alt Me. 11 (6), 380–385.
Meneses, M.M., Flores, M.E.M.J., 2019. Flavonoids: A promising therapy for obesity due to the high-fat diet. In: Flavonoids-A Coloring Model For Cheering Up Life.
Mosmann, T., 1983. Rapid colorimetric assay for cellular growth and survival: application to proliferation and cytotoxicity assays. J. Immunol. Methods 65 (1–2), 55–63.
Mutiso, S.K., Rono, D.K., Bukachi, F., 2014. Relationship between anthropometric measures and early electrocardiographic changes in obese rats. BMC Res. Notes. 7, 931.
Onat, A., Can, G., Kaya, H., Hergenç, G., 2010. "Atherogenic index of plasma" (log10 triglyceride/high- ensity lipoprotein-cholesterol) predicts high blood pressure, diabetes, and vascular events. J. Clin. Lipidol. 4 (2), 89–98.
Padwal, R.S., Majumdar, S.R., 2007. Drug treatments for obesity: orlistat, sibutramine, and rimonabant. The Lancet 369 (9555), 71–77.
Park, C.H., Yamabe, N., Noh, J.S., Kang, K.S., Tanaka, T., Yokozawa, T., 2009. The beneficial effects of morroniside on the inflammatory response and lipid metabolism in the liver of db/db mice. Biol. Pharm. Bull. 32 (10), 1734–1740.
Perry, R.J., Camporez, J.G., Kursawe, R., Titchenell, P.M., Zhang, D., 2015. Hepatic acetyl CoA links adipose tissue inflammation to hepatic insulin resistance and type 2 diabetes. Cell 160 (4), 745–758.
Pi-Sunyer, F.X., 2002. The obesity epidemic: pathophysiology and consequences of obesity. Obes. Res. 10 (2), 97–104.
Poirier, P., Giles, T.D., Bray, G.A., Hong, Y., Stern, J.S., Pi-Sunyer, F.X., Eckel, R.H., 2006. Obesity and cardiovascular disease: pathophysiology, evaluation, and effect of weight loss. Arterioscler. Thromb. Vasc. Biol. 26 (5), 968–976.
Ríos, J.L., 2011 May. Chemical constituents and pharmacological properties of Poria cocos. Planta Med. 77 (07), 681–691.
Samane, S., Noël, J., Charrouf, Z., Amarouch, H., Haddad, P.S., 2006. Insulin-sensitizing and anti-proliferative effects of Argania spinosa seed extracts. Evid Based Complement Alternat Med. 3 (3), 317–327.
Sato, M., Tai, T., Nunoura, Y., Yajima, Y., Kawashima, S., Tanaka, K., 2002. Dehydrotrametenolic acid induces preadipocyte differentiation and sensitizes animal models of noninsulin-dependent diabetes mellitus to insulin. Biol. Pharm. Bull. 25 (1), 81–86.
Sclafani, A., Springer, D., 1976. Dietary obesity in adult rats: similarities to hypothalamic and human obesity syndromes. Physiol. Behav. 17 (3), 461–471.
Shi, Y., Jiang, R., Liu, M., Fu, L., Zeng, G., Wan, Q., Mao, L., Deng, F., Zhang, X., Wei, Y., 2017. Facile synthesis of polymeric fluorescent organic nanoparticles based on the self-polymerization of dopamine for biological imaging. Mater. Sci. Eng.: C. 77 (1), 972–977.
Shi, Y., Liu, M., Deng, F., Zeng, G., Wan, Q., Zhang, X., Wei, Y., 2017. Recent progress and development on polymeric nanomaterials for photothermal therapy: a brief overview. J. Mater. Chem. B 5, 194–206.
Silha, J.V., Krsek, M., Skrha, J.V., Sucharda, P., Nyomba, B.L., Murphy, L.J., 2003. Plasma resistin, adiponectin and leptin levels in

lean and obese subjects: correlations with insulin resistance. Eur. J. Endocrinol. 149 (4), 331–335.

Sjöström, L., Narbro, K., Sjöström, C.D., Karason, K., Larsson, B., Wedel, H., Lystig, T., Sullivan, M., Bouchard, C., Carlsson, B., Bengtsson, C., Dahlgren, S., Gummesson, A., Jacobson, P., Karlsson, J., Lindroos, A.K., Lönroth, H., Näslund, I., Olbers, T., Stenlö, F.K., Torgerson, J., Agren, G., Carlsson, L.M., 2007. Effects of bariatric surgery on mortality in Swedish obese subjects. N. Engl. J. Med. 357, 741–752.

Surmi, B.K., Hasty, A.H., 2008. Macrophage infiltration into adipose tissue: initiation, propagation and remodeling. Future Lipidol. 3 (5), 545–556.

Tilg, H., Moschen, A.R., 2006. Adipocytokines: mediators linking adipose tissue, inflammation and immunity. Nat. Rev. Immunol. 6 (10), 772–783.

Titchenell, P.M., Quinn, W.J., Lu, M., Chu, Q., Lu, W., Li, C., Chen, H., Monks, B.R., Chen, J., Rabinowitz, J.D., Birnbaum, M.J., 2016. Direct hepatocyte insulin signaling is required for lipogenesis but is dispensable for the suppression of glucose production. Cell Metab. 23 (6), 1154–1166.

Tiwari, P.M., Vig, K., Dennis, V.A., Singh, S.R., 2011. Functionalized gold nanoparticles and their biomedical applications. Nanomaterials (Basel). 1 (1), 31–63.

Travers, M.E., McCarthy, M.T., 2011. Type 2 diabetes and obesity: Genomics and the clinic. Hum. Genet. 130 (1), 41–58.

Tsai, A.G., Williamson, D.F., Glick, H.A., 2011. Direct medical cost of overweight and obesity in the USA: a quantitative systematic review. Obes. Rev. 12 (1), 50–61.

Wahl, S., Drong, A., Lehne, B., Loh, M., 2017. Epigenome-wide association study of body mass index, and the adverse outcomes of adiposity. Nature 541 (7635), 81–86.

Wang, F., Wang, Y.C., Dou, S., Xiong, M.H., Sun, T.M., Wang, J., 2011. Doxorubicin-tethered responsive gold nanoparticles facilitate intracellular drug delivery for overcoming multidrug resistance in cancer cells. ACS Nano 5 (5), 3679–3692.

Warne, J.P., 2003. Tumour necrosis factor alpha: a key regulator of adipose tissue mass. J. Endocrinol. 177 (3), 351–355.

Warwick, Z.S., Schiffman, S.S., 1992. Role of dietary fat in calorie intake and weight gain. Neurosci. Biobehav. Rev. 16, 585–596.

Woods, S.C., Seeley, R.J., Rushing, P.A., D'Alessio, D., Tso, P., 2003. A controlled high-fat diet induces an obese syndrome in rats. J. Nut., 1331081–1331087

Yagi, K., 1978. Lipid peroxides and human disease. Chem. Physiol. Lipids 45, 337–351.

Zeng, G., Huang, L., Huang, Q., Liu, M., Xu, D., Huang, H., Yang, Z., Deng, F., Zhang, X., Wei, Y., 2018. Rapid synthesis of MoS_2-PDA-Ag nanocomposites as heterogeneous catalysts and antimicrobial agents via microwave irradiation. App. Surface Sci. 459 (30), 588–595.

Zhang, X., Huang, Q., Deng, F., Huang, H., Wan, Q., Liu, M., Wei, Y., 2017. Mussel-inspired fabrication of functional materials and their environmental applications: Progress and prospects. App Mater Today. 7, 222–238.

Zhou, W., Gao, X., Liu, D., Chen, X., 2015. Gold nanoparticles for in vitro diagnostics. Chem. Rev. 115 (19), 10575–10636.